HHS Public Access

Author manuscript

Biochemistry. Author manuscript; available in PMC 2018 April 11.

Published in final edited form as:

Biochemistry. 2017 February 28; 56(8): 1062–1074. doi:10.1021/acs.biochem.6b01020.

Perfluoro-*tert*-butyl Homoserine is a Helix-Promoting, Highly Fluorinated, NMR-Sensitive Aliphatic Amino Acid: Detection of the Estrogen Receptor•Coactivator Protein-Protein Interaction by ^{19}F NMR

Caitlin M. Tressler and **Neal J. Zondlo***

Department of Chemistry and Biochemistry, University of Delaware, Newark, Delaware 19716, United States

Abstract

Highly fluorinated amino acids can stabilize proteins and complexes with proteins, via enhanced hydrophobicity, and provide novel methods for identification of specific molecular events in complex solutions, via selective detection by ^{19}F NMR and the absence of native ^{19}F signals in biological contexts. However, the potential applications of ^{19}F NMR in probing biological processes are limited both by the strong propensities of most highly fluorinated amino acids for the extended conformation and by the relatively modest sensitivity of NMR spectroscopy, which typically constrains measurements to mid-micromolar concentrations. Herein, we demonstrate that perfluoro-*tert*-butyl homoserine exhibits a propensity for compact conformations, including α-helix and polyproline helix (PPII), that is similar to that of methionine. Perfluoro-*tert*-butyl homoserine has 9 equivalent fluorines that do not couple to any other nuclei, resulting in a sharp singlet that can be sensitively detected rapidly at low micromolar concentrations. Perfluoro-*tert*-butyl homoserine was incorporated at sites of leucine residues within the α-helical LXXLL short linear motif of estrogen receptor (ER) co-activator peptides. A peptide containing perfluoro-*tert*-butyl homoserine at the *i*+3 position of the ER coactivator LXX**L**L motif exhibited K_d = 2.2 μM for the estradiol-bound estrogen receptor, similar to that of the native ligand. ^{19}F NMR spectroscopy demonstrated the sensitive detection (5 μM concentration, 128 scans) of peptide binding to ER and of inhibition of protein-protein interaction by the native ligand or by the ER antagonist tamoxifen. These results suggest diverse potential applications of perfluoro-*tert*-butyl homoserine to probe protein function and protein-protein interfaces in complex solutions.

Graphical Abstract

*To whom correspondence should be addressed: zondlo@udel.edu, phone: +1-302-831-0197, fax +1-302-831-6335.

Supporting Information Available

^{1}H, ^{13}C, and ^{19}F NMR spectra of synthesized small molecules, CD spectra, and full synthesis and characterization data of all peptides, as well as additional ^{19}F NMR data. This material is available free of charge via the Internet at http://pubs.acs.org.

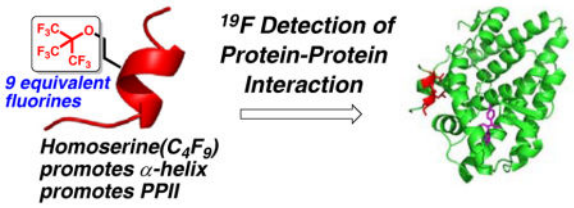

Keywords

^{19}F NMR; peptide structure; amino acids; secondary structure propensities; *tert*-butyl groups; protein-protein interactions; short linear motifs; theranostics

Introduction

Protein-protein interactions are central elements in both intracellular and extracellular signaling. Protein-protein interactions often involve intrinsically disordered proteins (IDPs), which frequently undergo a folding transition upon target binding.(1–6) Moreover, many protein-protein interactions important in intracellular signaling exhibit relatively modest affinities (high nanomolar to low micromolar dissociation constants (K_d)). Examples include transcriptional activation, protein kinase regulation via SH2 and SH3 domains, nuclear import and export, and recognition of ubiquitination targets by E3 ubiquitin ligases.(7–9) Many of these sites have their interaction strengths further modulated by post-translational modifications.(10–12) The modest strengths of these interactions have significant implications on intracellular dynamics. For example, a complex (A•B) with K_d = 1 μM (10^{-6} M) and a $k_{association}$ (A + B → A•B) = 10^6 M^{-1} s^{-1} yields $k_{dissociation}$ (A•B → A + B) = 1 s^{-1} ($K_d = k_{dissociation}/k_{association}$), resulting in a complex half-life of 0.7 seconds using these parameters (for a unimolecular dissociation, $t_{1/2} = 0.693/k_{dissociation}$). More generally, low micromolar dissociation constants (with $k_{association}$ values observed ranging from 10^3 to 10^9 M^{-1} s^{-1}) result in complex half-lives in the milliseconds to seconds time regime.(13–19) The rapid formation and dissociation of protein-protein complexes enable highly dynamic interaction networks, rapid responsiveness, and limited duration of responses to signaling. However, these interaction strengths and short lifetimes can pose significant complications for their identification and detection, particularly in complex milieu.

Protein-protein interactions play important roles in transcription. For example, the estrogen receptor (ER) is the central protein mediating cellular responsiveness to estrogens via transcription of estrogen-responsive genes. ER signaling is initiated by hormone binding to the ligand-binding domain (LBD), followed by dimerization of ER and import into the nucleus.(20, 21) Within the nucleus, the hormone-bound ER dimer binds DNA on estrogen-response elements (ERE). DNA binding is connected to transcription of estrogen-responsive genes via the recruitment of co-activator proteins associated with the transcriptional machinery. Co-activator proteins function via a transient protein-protein interaction employing a short amphipathic α-helix of the co-activator binding to the hormone-bound ER.(2, 3, 21–30) This protein-protein interaction both is central to ER-mediated transcription and is a potential therapeutic target for breast cancer.(31–38) Therefore, we

sought to develop peptides to probe binding of ligands and of co-activator proteins to ER, and to potentially disrupt this protein-protein interaction. In particular, we focused on ER co-activator peptides containing fluorine, due to fluorine's combination of hydrophobicity to facilitate binding and a nucleus observable by NMR spectroscopy and magnetic resonance imaging (MRI).

The high electronegativity, hydrophobicity, strong bonds, and small size of fluorine have resulted in the wide incorporation of fluorine in pharmaceuticals, polymers, and materials.(39) The electronegativity of fluorine also results in strong conformational effects associated with fluorine substitution.(40, 41) In addition to its physical properties, fluorine's major stable isotope, ^{19}F (100% natural abundance), is a spin-1/2 nucleus that is widely used for detection by NMR spectroscopy. ^{19}F has sensitivity by NMR that is similar to that of the ubiquitous ^{1}H. However, in contrast to hydrogen, the absence of ^{19}F in water, most organic solvents, and biological molecules renders ^{19}F a particularly sensitive probe due to the absence of background or competing signals from solvent or from other molecules.(42–44) These properties, combined with the wide (~300 ppm) chemical shift range of ^{19}F, have caused ^{19}F NMR, MRS, and MRI to be particularly useful in screening and in probing molecular function in environments as complex as cells and whole organisms.(45–68)

Numerous fluorinated amino acids have been developed to take advantage of the diverse structural and functional properties of fluorine (for a small subset, see Figure 1).(43, 69–76) Early work by the groups of Kumar, Marsh, and Tirrell demonstrated that coiled coil proteins with a fluorous hydrophobic core of trifluoroleucine or hexafluoroleucine exhibit both enhanced stability and self-sorting behavior due to the enhanced hydrophobic effect of fluorine.(77–83) These amino acids, as close analogues of leucine, can also be incorporated in expressed proteins, with either native or mutant LeuRS aminoacyl tRNA synthetases, opening their applications in protein engineering.(84, 85) Other fluorinated amino acids have been similarly employed to enhance stability and specificity in interactions via the hydrophobic effect or via conformational effects.(86–93) Expressed proteins containing fluorinated amino acids have also been employed to study protein folding in living cells.(54, 65, 67, 94)

Despite these and other successes, however, the fluorinated amino acids developed to date have two key potential limitations. First, most fluorinated amino acids strongly favor the extended conformation and strongly disfavor α-helical secondary structures: the enhanced stability of coiled coils with a hexafluoroleucine core occurs *despite* hexafluoroleucine *strongly* disfavoring the α-helical conformation, emphasizing the power of the enhanced hydrophobic effect of fluorine to overcome the strong bias against α-helix for this amino acid.(95–97) Similarly, trifluoro-Abu and pentafluorophenylalanine (Figure 1) exhibit substantially lower α-helix propensities than their non-fluorinated analogues ($\Delta\Delta G$ = +0.77 to +1.72 kcal mol^{-1}). Moreover, trifluorovaline, trifluoro-Abu, pentafluorophenylalanine, and fluorinated leucine analogues significantly stabilize the β-sheet.(74, 96–99) The α-helix represents 40% of the structure of folded proteins in the PDB; the development of highly fluorinated amino acids that favor the α-helix could potentially lead to stabilization via the hydrophobic or fluorophobic effect without the destabilizing effect of low α-helix propensity. Second, routine NMR spectroscopy is sensitive to only mid-micromolar

concentrations, while many key biological processes occur at lower concentrations. The incorporation of multiple fluorine atoms can lead to the ability to probe interactions at substantially lower concentrations or shorter observation times. However, the most heavily utilized highly fluorinated amino acids introduce additional limitations, including coupling to hydrogens (reducing signal-to-noise unless decoupling pulses are applied) and non-chemical equivalence of trifluoromethyl groups. For example, in hexafluoroleucine, the trifluoromethyl groups are diastereotopic, and thus typically exhibit two separate fluorine signals, each a doublet coupled to the methine hydrogen, substantially reducing sensitivity compared to what would be observed in a singlet of 6 equivalent fluorines.

In order to overcome these potential limitations and increase the sensitivity of peptides for detection by ^{19}F NMR, we are developing perfluoro-*tert*-butyl amino acids (Figure 1).(75, 100–104) Perfluoro-*tert*-butyl groups contain 9 chemically equivalent fluorines, with no coupled hydrogens, and thus present as a singlet in the ^{19}F NMR spectrum with a signal intensity of 9 fluorines. We previously described the synthesis of the diastereomeric amino acids 4*R*- and 4*S*-perfluoro-*tert*-butyl hydroxyproline, and demonstrated in peptides that they have divergent and predictable conformational preferences that depend on side chain stereochemistry. A peptide containing 4*R*-perfluoro-*tert*-butyl hydroxyproline was detected at 200 nM concentration in 5 minutes (128 scans, signal/noise = 7.2) by ^{19}F NMR, indicating the sensitivity gains possible with perfluoro-*tert*-butyl amino acids. However, while 4*R*-perfluoro-*tert*-butyl hydroxyproline strongly promotes polyproline helix, both amino acids were destabilizing at the N-terminus of α-helices relative to proline. Moreover, neither amino acid would be compatible with secondary structures employing hydrogen bonds via the main chain amide NH (e.g. beyond the first turn of an α-helix, or within a β-strand). Thus, we sought to develop alternative perfluoro-*tert*-butyl amino acids for applications in ^{19}F-based detection and imaging. Marsh and co-workers recently synthesized perfluoro-*tert*-butyl homoserine and demonstrated its compatibility with α-helices, using this amino acid to detect and control the interactions of amphipathic, hydrophobic α-helical peptides with membranes via its incorporation into antimicrobial peptides.(102) This amino acid is somewhat analogous to methionine, replacing the sulfur with an oxygen and the terminal methyl group with a perfluoro-*tert*-butyl group. Given the conformational preferences of methionine, which promotes both α-helix and polyproline helix (PPII), we sought to examine the use of perfluoro-*tert*-butyl homoserine within α-helical recognition epitopes and explore its use for the sensitive detection of protein-protein interactions by ^{19}F NMR.

Experimental

Small molecule synthesis

Synthetic procedures for the preparation of compounds **2–6** and characterization data (^{1}H NMR, ^{13}C NMR, and ^{19}F NMR spectra (where appropriate); high resolution mass spectrometry) are in the Supporting Information.

Peptide synthesis

Peptides containing perfluoro-*tert*-butyl homoserine were synthesized on NovaGel PEG-polystyrene graft Rink amide resin (0.67 mmol/g, EMD Millipore) by standard solid-phase peptide synthesis using HATU as a coupling reagent. The use of PEG-polystyrene graft resin resulted in substantially higher crude peptide purity than standard Rink amide polystyrene resin for the syntheses of peptides containing perfluoro-*tert*-butyl homoserine. Amide coupling reactions with Fmoc-perfluoro-*tert*-butyl homoserine (4 equivalents, 0.1 mmol scale) were allowed to proceed for 24 hours at room temperature. Subsequent amide coupling reactions were conducted as double-coupling reactions (2 hours for the first coupling, 1 hour for the second coupling). The NRBoxII peptide was synthesized using Rink amide polystyrene resin (0.7 mmol/g, 0.25 mmol, ChemImpex) with HBTU as a coupling reagent. All peptides were acetylated on the N-terminus (5% acetic anhydride in pyridine, 3 mL, 3 × 5 min) and contained a C-terminal amide. Synthesis, purification, and characterization details are in the Supporting Information.

Fluorescein Labeling

Peptides were labeled on the N-terminal cysteine using 5-iodoacetamidofluorescein (5-IAF) (Sigma-Aldrich). Purified peptides were dissolved in 250 mM phosphate buffer pH 4.0 (200 μL) and mixed with 10 mg/mL 5-IAF in DMF (200 μL) and the resultant solution incubated in the dark at room temperature for 90 minutes. The reaction mixtures were diluted with water (approximately 600 μL) and filtered before purification by HPLC. Purification and characterization details are in the Supporting Information

Circular dichroism

Circular dichroism (CD) experiments were completed on a Jasco model J-810 spectropolarimeter. All data were collected using a 1 mm cell (Starna Cells, Atascadero, CA). Data represent the average of at least 3 independent trials. Error bars indicate standard error. Data were background-corrected but were not smoothed. Experiments in Figure 2 were conducted at 25 °C. Experiments in Figure 3 and were conducted at 0.5 °C. The temperature for each experiment was chosen to allow direct comparison to the analogous peptides using previous data.(105, 106) Model peptides were also examined as a function of concentration, and exhibited no significant concentration-dependent change in CD signal between 6.2 μM and 50 μM (α-helical model peptide) or between 12.5 μM and 100 μM (PPII model peptide) (8-fold range in concentration for each) (Figures S2–S3).

Expression of the ERα LBD

A plasmid encoding the human estrogen receptor ligand-binding domain (ERα LBD) (amino acids 255-595) was obtained from the Koh lab at the University of Delaware. The ERα LBD expression construct was derived from pET-15b and contained a C-terminal Hexa-Histidine tag. The plasmid was transformed into BL21(DE3) pLysS competent cells (Novagen) using heat shock and grown overnight at 37 °C on luria broth (LB) media containing 50 mg/L ampicillin. A single colony was selected and grown overnight at 37 °C in 100 mL LB media containing 50 mg/L ampicillin. Terrific broth expression cultures with 50 mg/L ampicillin were inoculated with 25–30 mL of the overnight culture and grown to an

optical density of 0.6 to 0.8. Cultures were induced with 1 mM IPTG for 5 hours before centrifugation. Bacterial cell pellets were frozen at −20 °C until purification. ERα LBD was purified using His-Bind resin (EMD Millipore) according to the manufacturer's directions, with 200 μM PMSF and 10 μM estradiol added to the binding buffer. Protein identity was verified by SDS-PAGE and MALDI MS. Protein eluents were dialyzed into phosphate-buffered saline (PBS) at pH 7.4 with 5 mM EDTA and 0.5 mM DTT, and protein concentration determined via Bradford assay.

Fluorescence polarization

Peptides and ERα LBD were diluted in 1× PBS buffer (140 mM NaCl, 2.7 mM KCl, 10 mM K_2HPO_4, 2 mM KH_2PO_4) pH 7.4. Peptide concentrations were determined by absorbance at 492 nm using a fluorescein extinction coefficient of 83,000. Fluorescence polarization assays were conducted in 96 well round-bottom black opaque plates (Costar) using two-fold serial dilutions of ERα LBD to final protein concentrations from 10 μM to 0.0098 μM in PBS containing 0.1 mM DTT, 20 μM 17β-estradiol, 0.04 mg/mL BSA, and 100 nM fluorescein-labeled peptide. Solutions were incubated in the dark for 30 minutes at room temperature before reading on a Perkin-Elmer Fusion plate reader using a 485 nm fluorescein excitation filter and a 535 nm emission filter with polarizer. All data are the average of at least three independent trials. All dissociation constants (K_d) were determined using a nonlinear least-squares curve fit (KaleidaGraph 4.1) of the K_d to the fluorescence polarization data, via a quadratic binding equation for 1:1 complex formation. All data were fit using equation 1, where p_{min} = the polarization value without protein present, p_{max} = polarization at saturation.

$$\text{polarization} = p_{\min} + (p_{\max} - p_{\min}) \times \frac{([\text{ligand}]_{\text{total}} + [\text{protein}]_{\text{total}} + K_d) - \sqrt{(([\text{ligand}]_{\text{total}} + [\text{protein}]_{\text{total}} + K_d)^2 - 4[\text{ligand}]_{\text{total}}[\text{protein}]_{\text{total}}])}}{2[\text{ligand}]_{\text{total}}} \quad (1)$$

^{1}H NMR spectroscopy

Peptides were characterized by ^{1}H NMR spectroscopy in 5 mM phosphate buffer (pH 4) with 25 mM NaCl in 90% H_2O/10% D_2O and analyzed as described previously.(100, 104–106) The coupling constant $^3J_{\alpha N}$, which correlates with the ϕ torsion angle via a parametrized Karplus equation,(107) was calculated for perfluoro-*tert*-butyl homoserine in peptides in order to directly examine the effects of this amino acid on ϕ in different peptide contexts. Resonance assignments were obtained via TOCSY spectra. TOCSY spectra and ^{1}H-^{13}C HSQC spectra were also recorded in order to determine the effects of Hse(C_4F_9) substitution on conformation in the peptides NRBoxII and Leu12Hse(C_4F_9), via analysis of changes in Hα, Hβ, and ^{13}Cα chemical shift, which correlate with main chain conformation.

(108–110) These experiments indicated minimal structural perturbation within the α-helical NRBoxII peptide due to substitution of leucine with perfluoro-*tert*-butyl homoserine. See the Supporting Information for details.

^{19}F NMR spectroscopy

Peptide concentrations were determined by ^{1}H NMR spectroscopy using 1 mM maleic acid as a standard. Peptides and protein were diluted in 1× PBS (140 mM NaCl, 2.7 mM KCl, 10 mM K_2HPO_4, 2 mM KH_2PO_4) pH 7.4 with 0.1 mM DTT and 20 μM 17β-estradiol to a final volume of 500 μL. For the peptide competition experiments, NMR spectra were initially recorded in the absence of NRBoxII peptide. NRBoxII peptide was added (< 5 μL) and the resultant solution was allowed to equilibrate for a minimum of 30 minutes at room temperature before the NMR experiment was conducted. For experiments containing 4-hydroxytamoxifen (OHT), 50 μM OHT was added to the solution instead of estradiol. The Leu12Hse(C_4F_9) peptide concentration in all NMR experiments was 5 μM. All NMR samples contained 10% D_2O. Solutions were allowed to incubate at room temperature for at least 30 minutes to equilibrate. Data were recorded on a Brüker 600 MHz (^{19}F 564.5 MHz) NMR spectrometer equipped with a 5-mm Brüker SMART probe using a standard zg pulse sequence without proton decoupling. A 0.8 second acquisition time was used with a 3 second relaxation delay and a 10 ppm sweep width. NMR data were zero-filled to 64K data points and processed with an exponential multiplication apodization function with 2.0 Hz line broadening, unless otherwise indicated. Peak widths (full width at half height, FWHH) were calculated using the peak analysis calculator in Mnova 10.

Results

Fmoc-perfluoro-*tert*-butyl homoserine was synthesized in a compact approach from the inexpensive amino acid homoserine (Scheme 1). This synthetic route is similar to that developed by Marsh;(102) key differences include avoiding the use of diazomethane for methyl ester protection, employing HCl in place of TFA for Boc deprotection, and the use of Fmoc-OSu for Fmoc protection. The key step of the synthesis is the Mitsunobu reaction of the homoserine side chain alcohol with perfluoro-*tert*-butanol, as was used previously in the synthesis of perfluoro-*tert*-butyl hydroxyprolines and other described perfluoro-*tert*-butyl ethers.(75, 100–102, 111)

To examine the inherent conformational preferences of perfluoro-*tert*-butyl homoserine, this amino acid was incorporated into a Baldwin-type α-helical model peptide used previously to identify the effects of serine and threonine phosphorylation and O-GlcNAcylation on α-helix stability.(106, 112, 113) At the N-terminus of α-helices, proline is helix-stabilizing due to conformational restriction and the absence of a requirement for hydrogen-bond donors, which are solvent-exposed here.(114–117) However, we previously observed that both 4*R*- and 4*S*- perfluoro-*tert*-butyl hydroxyproline destabilize the α-helix at this position, relative to proline (Table 1).(100) In contrast, perfluoro-*tert*-butyl homoserine exhibited α-helicity similar to that of proline at this position (Figure 2). Previous work by Doig in a closely related model system (Ac-**X**AAAAQAAAAQAAGY-NH_2) demonstrated that proline and methionine have similar α-helix propensities at the N-terminus of α-helices.(116) These

data indicate that perfluoro-*tert*-butyl homoserine has a similar propensity for α-helicity at this position as its nearest non-fluorinated native amino acid analogue, methionine. In contrast, for all other highly fluorinated amino acids examined to date, fluorination results in a substantial *reduction* in α-helix propensity.(74, 95–97) For non-polar non-proline amino acids, α-helix propensity is typically similar at different locations within the α-helix, (118) although herein we did not examine the effect of perfluoro-*tert*-butyl homoserine in a central position of an α-helix. The low α-helix propensity of highly fluorinated amino acids has been previously ascribed to the presence of the solvophobic and more sterically demanding fluorine atom(s) near the polar peptide backbone, promoting a more extended conformation. (74, 95, 96, 98) The data herein suggest that perfluoro-*tert*-butyl homoserine might find special applications as a fluorinated amino acid that *stabilizes*, rather than significantly *destabilizes*, α-helices.

The polyproline II helix (PPII) conformation is widely recognized for its roles in globular proteins, at protein-protein interfaces, and in the unfolded state.(119–122) PPII exhibits a relatively compact value of ϕ, but a more extended value of ψ (average ϕ, ψ = (−75°, +145°)), and is considered a bridge between fully compact (e.g. α-helix) and extended (e.g. β-sheet) conformations. Due to the possibility of a steric clash between the side chain and that of the subsequent residue, sterically hindered amino acids strongly disfavor PPII conformation.(105, 123–125) While we are unaware of any examination of PPII propensities of highly fluorinated non-proline amino acids, these observations suggest that they might disfavor PPII for similar reasons to those causing their low α-helix propensities.

Perfluoro-*tert*-butyl homoserine was incorporated at the guest position (**X**) in a model peptide (Ac-GPP**X**PPGY-NH_2) context previously employed to identify the PPII propensities of all canonical amino acids and a series of unnatural amino acids.(105, 126) Perfluoro-*tert*-butyl homoserine exhibited one of the higher PPII propensities among studied amino acids (Figure 3, Table 2). The PPII propensity of perfluoro-*tert*-butyl homoserine was significantly lower than that of proline or leucine, but was similar to that of methionine, lysine, and arginine, as well as homoserine. Notably, the PPII propensity of perfluoro-*tert*-butyl homoserine was significantly greater than that of the sterically hindered β-branched amino acids valine, threonine, isoleucine, or *tert*-leucine. We previously postulated that the high PPII propensity of Leu, but low PPII propensities of its isomers isoleucine and *tert*-leucine, was due to the strong rotameric preferences (e.g. the avoidance of *syn*-pentane interactions) of leucine that keep the terminal methyl groups away from the protein backbone.(127, 128) This hypothesis also explains the high PPII propensities of longer-chain amino acids methionine, arginine, and lysine. Combined, these data suggest that the good propensities of perfluoro-*tert*-butyl homoserine for both α-helix and PPII might be due to strong side chain conformational preferences that keep the sterically demanding perfluoro-*tert*-butyl group away from the peptide backbone. In contrast, for other heavily fluorinated amino acids (e.g. trifluoroleucine, trifluorovaline, hexafluoroleucine, trifluoro-Abu (Figure 1)), the steric and/or solvation energetic cost associated with the fluorines being located near the backbone leads to a strong preference *against* compact conformations.(95–97) The data herein establish perfluoro-*tert*-butyl homoserine as an unusual highly fluorinated amino acid that prefers *compact* conformations (α-helix, PPII).

To examine the potential application of perfluoro-*tert*-butyl homoserine to molecular recognition via α-helices, and its use as a probe of relatively weak protein-protein interactions by ^{19}F NMR, this amino acid was incorporated into the recognition α-helix of the estrogen receptor co-activator NRBoxII peptide (Figure 4).(20–22) DNA-bound ER induces transcription via recruitment of co-activator proteins that bind to the ligand-bound ER via short amphipathic α-helices (indicated in red in Figure 4) that include an LXXLL short linear motif.(2, 3, 21–29) Excess estrogen-mediated signaling has a causative role in many breast cancers. Inhibition of estrogen signaling can be achieved through direct inhibition of hormone binding, via clinical agents such as tamoxifen. Alternatively, estrogen signaling can additionally by inhibited by disruption of the binding of co-activators to the ligand-bound ER, which has been achieved via peptides and small molecules.(30–38) A peptide that binds to the ligand-bound ER and that contains a handle for molecular detection and functional interrogation thus has bifunctional potential in both therapeutics and in imaging/diagnostics (a so-called theranostic agent).

Peptides were synthesized based on ligands of the well-studied NRBox II coactivator sequence (Figure 4). Examination of the crystal structure of this coactivator with ligand-bound ERα indicated that residues Leu9 (*i* position of the **L**XXLL motif) and Leu12 (*i*+3 position, LXX**L**L) of the coactivator might accommodate the larger perfluoro-*tert*-butyl homoserine amino acid.(22) In contrast, Leu13 (*i*+4 position, LXXL**L**) is deeply buried in the co-crystal structure and was not expected to tolerate substitution with perfluoro-*tert*-butyl homoserine. In addition, Ile8 (*i*–1 position) makes a hydrophobic contact with ERα but is significantly solvent-exposed, suggesting that it could also be a site of substitution. Notably, Spatola and co-workers had previously demonstrated substantially enhanced ERα affinity of coactivator peptides in which either the *i* or *i*+3 leucine was replaced by the larger and more hydrophobic residue neopentylglycine, with the highest affinity ligand resulting from substitution at the *i*+3 leucine.(129)

Therefore, peptides were synthesized in which each of Ile8, Leu9, and Leu12 of NRBoxII was replaced with perfluoro-*tert*-butyl homoserine (Figure 4). In addition, as a negative control, Leu9 was replaced with 4*S*-perfluoro-*tert*-butyl hydroxyproline. This amino acid is expected to significantly destabilize the recognition α-helix(100) while containing the perfluoro-*tert*-butyl group and still being able to be adopt an α-helix (substitution of a proline at the *i*+3 or *i*+4 residues would prevent α-helix formation). Thus, the peptide Leu9hyp(C_4F_9) provides a control for the effect of the hydrophobic perfluoro-*tert*-butyl group on coactivator binding.(130)

All peptides were site-specifically labeled on cysteine with 5-iodoacetamidofluorescein and their binding affinities for the estradiol-bound ERα LBD determined by direct fluorescence polarization assays (Figure 5).(31) The NRBoxII peptide exhibited an affinity for ERα•estradiol of 1.0 μM, comparable to that observed previously. The peptide Leu12Hse(C_4F_9) exhibited an affinity similar to that of the native ligand (K_d = 2.2 μM), consistent with the design and indicating the ability to incorporate perfluoro-*tert*-butyl homoserine at a recognition residue in a protein-protein interface (Table 3). Notably, alanine substitution at this position results in a 19-fold loss in ERα affinity, suggesting direct engagement of perfluoro-*tert*-butyl homoserine at the binding site.(131) Ile8Hse(C_4F_9)

substitution also was tolerated in the complex, with a modest 1.2 kcal mol^{-1} loss in binding energy compared to the native ligand. In contrast, the peptide Leu9Hse(C_4F_9) exhibited a substantial loss in affinity, indicating lesser tolerance for the larger perfluoro-*tert*-butyl homoserine at this position. As expected, the peptide hyp9Hse(C_4F_9) exhibited only a weak interaction with ERα•estradiol, indicating that the interactions of other peptides were not driven solely by the hydrophobicity of the perfluoro-*tert*-butyl group. Collectively, these data indicate that perfluoro-*tert*-butyl homoserine can be accommodated at a site of molecular recognition within an α-helical recognition epitope of a protein-protein interaction.

In view of its near-native affinity for estradiol-bound ERα, the peptide Leu12Hse(C_4F_9) was further examined for the ability to detect the ERα•coactivator protein-protein interaction in solution by ^{19}F NMR. Notably, the affinity observed for this complex (low μM) is similar to that of many affinities of protein-protein interactions involving intrinsically disordered proteins important in cell signaling.(2, 3, 7, 28, 29, 132) At 5 μM peptide concentration in aqueous solution, the peptide Leu12Hse(C_4F_9) exhibited a singlet peak (full width at half height (FWHH) = 6 Hz) by ^{19}F NMR (Figure 6a). This peptide could be detected with good signal-to-noise in only 128 scans (8 minute experiment, Figure S22).(133) Titration of the ERα LBD resulted in broadening of the ^{19}F signal associated with complex formation (Figure 6b–d, FWHH = 18 Hz at [ERα] = 15 μM), which was used to determine the K_d of this peptide-protein interaction by ^{19}F NMR under these solution conditions (K_d = 2.9 ± 0.8 μM, similar to that observed by fluorescence polarization; see the Supporting Information for details). This observed peak broadening could be due to dynamic exchange or to chemical shift anisotropy (CSA) via the large size of the ERα protein (39 kDa) increasing the rotational correlation time of the complex.(42, 45, 49) Importantly, the broadening induced by the ERα protein is not due to non-specific interactions: addition of bovine gamma globulin (155 kDa) at similar concentrations resulted in no induced anisotropy in the ^{19}F NMR spectrum (Figure 6e).

The observed ^{19}F broadening due to Leu12Hse(C_4F_9)•ERα peptide•protein complex formation was reversed by the addition of the competitive native ligand NRBoxII peptide, with reappearance of the sharp singlet of Leu12Hse(C_4F_9) in the ^{19}F NMR spectrum (Figure 6f (FWHH = 6 Hz) versus Figure 6c (FWHH = 18 Hz)). These data indicate the use of a peptide containing perfluoro-*tert*-butyl homoserine to interrogate the ERα•coactivator protein-protein interaction at concentrations similar to the K_d of the complex, and suggest broader potential application of perfluoro-*tert*-butyl amino acids in probing protein-protein interactions at physiologically relevant concentrations. Moreover, addition of the estrogen receptor antagonist tamoxifen to the ERα•Leu12Hse(C_4F_9) complex resulted in the reduction of ^{19}F broadening (Figure 6c (15 μM ERα, no tamoxifen, FWHH = 18 Hz) versus Figure 6g (15 μM ERα plus 50 μM tamoxifen, FWHH = 9 Hz). Finally, this peptide•protein interaction was examined in the complex medium of HeLa cell extracts. The peptide Leu12Hse(C_4F_9) was observed at 5 μM as a singlet in HeLa cell extracts in the absence of ERα (Figure 6h). Modest broadening of the peak was observed in cell extracts (FWHH = 10 Hz) compared to buffered aqueous solution, as has been observed previously in experiments in cell extracts and cells.(54, 65, 67, 94) An increase in broadening was observed on the addition of ERα (Figure 6i, FWHH = 21 Hz), as had been observed in simple buffered aqueous solutions (Figures 6a and 6c). These results indicate the utility of perfluoro-*tert*-

butyl homoserine to identify a protein-protein interaction at low micromolar concentration by ^{19}F NMR even in the highly complex media of cell extracts. Collectively, these data suggest divergent uses of perfluoro-*tert*-butyl amino acids, including in the sensitive and specific screening of peptide and small molecule inhibitors of protein function and protein-protein interactions in complex solutions.(8, 60, 62, 134, 135)

Discussion

Fluorinated amino acids in peptides and proteins have outstanding potential in protein engineering, protein design, studies on protein dynamics, structure-function analysis of proteins in solution and in cells, and biomedical imaging.(43, 44, 46, 47, 49, 54, 56, 60, 61, 64, 136–138) Fluorinated amino acids transcend many typical challenges of NMR spectroscopy in complex solutions via spectral simplification (eliminating challenges in assignment) and limited background signal (no native ^{19}F signals) compared to standard techniques that must compete against ubiquitous ^{1}H resonances present in proteins, metabolites, and water, and in heteronuclear NMR against competing ^{13}C and ^{15}N nuclei present at natural abundance. However, most highly fluorinated amino acids described to date have two key potential limitations, modest sensitivity and strong conformational preferences against compact conformations.

NMR spectroscopy is inherently a technique of relatively modest sensitivity, typically requiring mid-micromolar or higher concentrations. Sensitivity in NMR is most effectively improved by increasing the concentrations of signals: an increase from 1 to 3 chemically equivalent signals (a 3-fold increase in signal concentration) results in a 3-fold increase in sensitivity and a 9-fold decrease in the experimental time required to achieve a given signal-to-noise at a given concentration. Thus, at a given concentration, a trifluoromethyl (n = 3) group will be observed at a given signal-to-noise in 1/9 ($1/n^2$) the amount of experimental time as the same molecule with only a single fluorine (n = 1). In the amino acids hexafluoroleucine or hexafluorovaline, however, the potential benefits of signal increase are reduced because each trifluoromethyl group is diastereotopic and exhibits a separate resonance. Moreover, each resonance is further reduced in intensity via coupling to the methine hydrogen. Thus, while exhibiting substantial increases in sensitivity over molecules with only a single fluorine, this potential benefit is reduced due to stereochemical considerations and scalar coupling. In contrast, perfluoro-*tert*-butyl homoserine contains 9 *chemically equivalent fluorines* that *do not couple to any other nuclei*, and thus exhibits a singlet with a signal intensity 9× that of a single (uncoupled) fluorine, capable of achieving comparable signal-to-noise at a given concentration in 1/81 the amount of experimental time. The substantial increase in sensitivity has the potential to significantly reduce the concentrations accessible for analysis by ^{19}F NMR to those relevant for dynamic protein-protein interactions that are central to signal transduction. This increase in sensitivity for perfluoro-*tert*-butyl homoserine also suggests potential future applications in the molecular analysis of protein function in cells and *in vivo*.

All highly fluorinated amino acids that have been examined previously have been found to exhibit a strong preference against the α-helix conformation and for the extended conformation. These conformational preferences have been exploited in the design of

proteins with stabilized β-sheets and in the development of amyloid-inducing peptide sequences via sequential amino acid fluorination.(95–97, 99) Herein, we have demonstrated that perfluoro-*tert*-butyl homoserine exhibits excellent propensity for both α-helix and polyproline helix conformations, comparable to the related canonical amino acid methionine. These data suggest the specific potential application of perfluoro-*tert*-butyl homoserine in the design of highly stabilized helical proteins stabilized by fluorination, as well as the application of perfluoro-*tert*-butyl homoserine at α-helical interfaces, to achieve increased affinity via the enhanced hydrophobic effect of fluorine but without the previously observed energetic penalty of low α-helical propensity of highly fluorinated amino acids.

The propensity for more compact conformations, including polyproline helix, for perfluoro-*tert*-butyl homoserine also suggests potential applications in probing function of intrinsically disordered proteins (IDPs). IDPs have central roles in cell signaling and in protein-protein interactions, including in transcription, often via disorder-to-order transitions on complex formation.(4–6, 9) IDPs often exhibit protein-protein interactions with modest affinities, which allows for rapid changes in protein function and for responsive, dynamic protein switches. These modest affinities and dynamic interactions, however, pose challenges for the structural and functional characterization of IDPs.(10–12, 139, 140) The work herein suggests potential applications of perfluoro-*tert*-butyl amino acids in probing function, protein-protein interactions, and post-translational modifications of IDPs in complex environments, including cells. The sensitivity gains of perfluoro-*tert*-butyl amino acids combined with their ready incorporation in biologically active molecules also suggest their potential clinical application in magnetic resonance spectroscopy (MRS) and magnetic resonance imaging (MRI).

Conclusion

We have synthesized Fmoc-perfluoro-*tert*-butyl homoserine and incorporated this amino acid into both model peptides and into intrinsically disordered coactivator peptide ligands of the estrogen receptor. Perfluoro-*tert*-butyl homoserine exhibits high propensity for both the α-helix and polyproline helix conformations. This propensity for compact conformations stands in contrast to all other highly fluorinated amino acids investigated to date. An α-helical estrogen receptor coactivator peptide containing perfluoro-*tert*-butyl homoserine at the site of a recognition leucine exhibited similar affinity as the native ligand for estradiol-bound estrogen receptor, indicating the ability of perfluoro-*tert*-butyl homoserine to function as a mimic of hydrophobic aliphatic amino acids at sites where the greater size of perfluoro-*tert*-butyl homoserine can be accommodated. This peptide allowed detection by ^{19}F NMR of protein-protein interactions and inhibition of protein function by small molecules in rapid experiments at low micromolar concentration. These data suggest broad potential applications of perfluoro-*tert*-butyl amino acids in protein design and in probing protein structure, function, and dynamics in complex environments.

Supplementary Material

Refer to Web version on PubMed Central for supplementary material.

Acknowledgments

We thank NSF (CHE-1412978) and NIH (GM93225) for funding. Instrumentation support was provided by NIH (GM110758) and NSF (CHE-1229234). We thank John Koh for the plasmid encoding ERα and for helpful discussions.

References

1. Tompa P, Schad E, Tantos A, Kalmar L. Intrinsically disordered proteins: emerging interaction specialists. Curr Opin Struct Biol. 2015; 35:49–59. [PubMed: 26402567]
2. Van Roey K, Uyar B, Weatheritt RJ, Dinkel H, Seiler M, Budd A, Gibson TJ, Davey NE. Short Linear Motifs: Ubiquitous and Functionally Diverse Protein Interaction Modules Directing Cell Regulation. Chem Rev. 2014; 114:6733–6778. [PubMed: 24926813]
3. Davey NE, Van Roey K, Weatheritt RJ, Toedt G, Uyar B, Altenberg B, Budd A, Diella F, Dinkel H, Gibson TJ. Attributes of short linear motifs. Mol BioSyst. 2012; 8:268–281. [PubMed: 21909575]
4. Uversky VN, Oldfield CJ, Dunker AK. Showing your ID: intrinsic disorder as an ID for recognition, regulation and cell signaling. J Mol Recognit. 2005; 18:343–384. [PubMed: 16094605]
5. Tompa P, Fuxreiter M, Oldfield CJ, Simon I, Dunker AK, Uversky VN. Close encounters of the third kind: disordered domains and the interactions of proteins. Bioessays. 2009; 31:328–335. [PubMed: 19260013]
6. Oldfield CJ, Cheng YG, Cortese MS, Romero P, Uversky VN, Dunker AK. Coupled folding and binding with alpha-helix-forming molecular recognition elements. Biochemistry. 2005; 44:12454–12470. [PubMed: 16156658]
7. Ball LJ, Kuhne R, Schneider-Mergener J, Oschkinat H. Recognition of proline-rich motifs by protein-protein-interaction domains. Angew Chem Int Ed. 2005; 44:2852–2869.
8. Milroy LG, Grossmann TN, Hennig S, Brunsveld L, Ottmann C. Modulators of Protein-Protein Interactions. Chem Rev. 2014; 114:4695–4748. [PubMed: 24735440]
9. Liu J, Perumal NB, Oldfield CJ, Su EW, Uversky VN, Dunker AK. Intrinsic Disorder in Transcription Factors. Biochemistry. 2006; 45:6873–6888. [PubMed: 16734424]
10. Theillet FX, Smet-Nocca C, Liokatis S, Thongwichian R, Kosten J, Yoon MK, Kriwacki RW, Landrieu I, Lippens G, Selenko P. Cell signaling, post-translational protein modifications and NMR spectroscopy. J Biomol NMR. 2012; 54:217–236. [PubMed: 23011410]
11. Theillet FX, Binolfi A, Frembgen-Kesner T, Hingorani K, Sarkar M, Kyne C, Li CG, Crowley PB, Gierasch L, Pielak GJ, Elcock AH, Gershenson A, Selenko P. Physicochemical Properties of Cells and Their Effects on Intrinsically Disordered Proteins (IDPs). Chem Rev. 2014; 114:6661–6714. [PubMed: 24901537]
12. Lippens G, Landrieu I, Hanoulle X. Studying Posttranslational modifications by in-cell NMR. Chem Biol. 2008; 15:311–312. [PubMed: 18420137]
13. Sugase K, Dyson HJ, Wright PE. Mechanism of coupled folding and binding of an intrinsically disordered protein. Nature. 2007; 447:1021-U1011. [PubMed: 17522630]
14. Demers JP, Mittermaier A. Binding Mechanism of an SH3 Domain Studied by NMR and ITC. J Am Chem Soc. 2009; 131:4355–4367. [PubMed: 19267471]
15. Schreiber G, Haran G, Zhou HX. Fundamental Aspects of Protein-Protein Association Kinetics. Chem Rev. 2009; 109:839–860. [PubMed: 19196002]
16. Zhou HX, Pang XD, Lu C. Rate constants and mechanisms of intrinsically disordered proteins binding to structured targets. Phys Chem Chem Phys. 2012; 14:10466–10476. [PubMed: 22744607]
17. Dogan J, Jonasson J, Andersson E, Jemth P. Binding Rate Constants Reveal Distinct Features of Disordered Protein Domains. Biochemistry. 2015; 54:4741–4750. [PubMed: 26153298]
18. Wright PE, Dyson HJ. Intrinsically disordered proteins in cellular signalling and regulation. Nat Rev Mol Cell Biol. 2015; 16:18–29. [PubMed: 25531225]
19. Gianni S, Dogan J, Jemth P. Coupled binding and folding of intrinsically disordered proteins: what can we learn from kinetics? Curr Opin Struct Biol. 2016; 36:18–24. [PubMed: 26720267]

20. Tenbaum S, Baniahmad A. Nuclear Receptors: Structure, Function and Involvement in Disease. Int J Biochem Cell Biol. 1997; 29:1325–1341. [PubMed: 9570131]
21. Steinmetz ACU, Renaud JP, Moras D. Binding of Ligands and Activation of Transcription by Nuclear Receptors. Annu Rev Biophys Biomol Struct. 2001; 30:329–359. [PubMed: 11340063]
22. Shiau AK, Barstad D, Loria PM, Cheng L, Kushner PJ, Agard DA, Greene GL. The structural basis of estrogen receptor-coactivator recognition and antagonism of this interaction by tamoxifen. Cell. 1998; 95:927–937. [PubMed: 9875847]
23. Tamrazi A, Carlson KE, Rodriguez AL, Katzenellenbogen JA. Coactivator proteins as determinants of estrogen receptor structure and function: Spectroscopic evidence for a novel coactivator-stabilized receptor conformation. Mol Endocrinol. 2005; 19:1516–1528. [PubMed: 15661830]
24. Jeyakunnar M, Carlson KE, Gunther JR, Katzenellenbogen JA. Exploration of Dimensions of Estrogen Potency PARSING LIGAND BINDING AND COACTIVATOR BINDING AFFINITIES. J Biol Chem. 2011; 286:12971–12982. [PubMed: 21321128]
25. Darimont BD, Wagner RL, Apriletti JW, Stallcup MR, Kushner PJ, Baxter JD, Fletterick RJ, Yamamoto KR. Structure and Specificity of nuclear receptor-coactivator interactions. Genes Dev. 1998; 12:3343–3356. [PubMed: 9808622]
26. Johnson AB, O'Malley BW. Steroid receptor coactivators 1, 2, and 3: Critical regulators of nuclear receptor activity and steroid receptor modulator (SRM)-based cancer therapy. Mol Cell Endocrinol. 2012; 348:430–439. [PubMed: 21664237]
27. Fuchs S, Nguyen HD, Phan TTP, Burton MF, Nieto L, de Vries-van Leeuwen IJ, Schmidt A, Goodarzifard M, Agten SM, Rose R, Ottmann C, Milroy LG, Brunsveld L. Proline Primed Helix Length as a Modulator of the Nuclear Receptor-Coactivator Interaction. J Am Chem Soc. 2013; 135:4364–4371. [PubMed: 23437920]
28. Lee Y, Sampson NS. Romping the cellular landscape: linear scaffolds for molecular recognition. Curr Opin Struct Biol. 2006; 16:544–550. [PubMed: 16781140]
29. Diella F, Haslam N, Chica C, Budd A, Michael S, Brown NP, Trave G, Gibson TJ. Understanding eukaryotic linear motifs and their role in cell signaling and regulation. Front Biosci. 2008; 13:6580–6603. [PubMed: 18508681]
30. Margeat E, Bourdoncle A, Margueron R, Poujol N, Cavailles V, Royer C. Ligands differentially modulate the protein interactions of the human estrogen receptors alpha and beta. J Mol Biol. 2003; 326:77–92. [PubMed: 12547192]
31. Becerril J, Hamilton AD. Helix Mimetics as Inhibitors of the Interaction of the Estrogen Receptor with Coactivator Peptides. Angew Chem, Int Ed. 2007; 46:4471–4473.
32. Gunther JR, Moore TW, Collins ML, Katzenellenbogen JA. Amphipathic benzenes are designed inhibitors of the estrogen receptor alpha/steroid receptor coactivator interaction. ACS Chem Biol. 2008; 3:282–286. [PubMed: 18484708]
33. Parent AA, Gunther JR, Katzenellenbogen JA. Blocking Estrogen Signaling After the Hormone: Pyrimidine-Core Inhibitors of Estrogen Receptor-Coactivator Binding. J Med Chem. 2008; 51:6512–6530. [PubMed: 18785725]
34. Williams AB, Weiser PT, Hanson RN, Gunther JR, Katzenellenbogen JA. Synthesis of Biphenyl Proteomimetics as Estrogen Receptor-alpha Coactivator Binding Inhibitors. Org Lett. 2009; 11:5370–5373. [PubMed: 19902964]
35. Phan T, Nguyen HD, Goksel H, Mocklinghoff S, Brunsveld L. Phage display selection of miniprotein binders of the Estrogen Receptor. Chem Commun. 2010; 46:8207–8209.
36. Phillips C, Roberts LR, Schade M, Bazin R, Bent A, Davies NL, Moore R, Pannifer AD, Pickford AR, Prior SH, Read CM, Scott A, Brown DG, Xu B, Irving SL. Design and Structure of Stapled Peptides Binding to Estrogen Receptors. J Am Chem Soc. 2011; 133:9696–9699. [PubMed: 21612236]
37. Shapiro DJ, Mao CJ, Cherian MT. Small Molecule Inhibitors as Probes for Estrogen and Androgen Receptor Action. J Biol Chem. 2011; 286:4043–4048. [PubMed: 21149443]
38. Sun AM, Moore TW, Gunther JR, Kim MS, Rhoden E, Du YH, Fu HA, Snyder JP, Katzenellenbogen JA. Discovering Small-Molecule Estrogen Receptor alpha/Coactivator Binding Inhibitors: High-Throughput Screening, Ligand Development, and Models for Enhanced Potency. ChemMedChem. 2011; 6:654–666. [PubMed: 21365764]

39. Muller K, Faeh C, Diederich F. Fluorine in pharmaceuticals: Looking beyond intuition. Science. 2007; 317:1881–1886. [PubMed: 17901324]
40. Hamman S, Beguin C, Charlon C, Luuduc C. Conformational Studies on 2-Fluoro-1,2-Disubstituted Ethanes by Nmr-Spectroscopy - Influence of Electronegativity on Vicinal Proton Proton and Fluorine Proton Coupling-Constants. Org Magn Resonance. 1983; 21:361–366.
41. Zimmer LE, Sparr C, Gilmour R. Fluorine Conformational Effects in Organocatalysis: An Emerging Strategy for Molecular Design. Angew Chem, Int Ed. 2011; 50:11860–11871.
42. Dalvit C, Fagerness PE, Hadden DTA, Sarver RW, Stockman BJ. Fluorine-NMR experiments for high-throughput screening: Theoretical aspects, practical considerations, and range of applicability. J Am Chem Soc. 2003; 125:7696–7703. [PubMed: 12812511]
43. Ruiz-Cabello J, Barnett BP, Bottomley PA, Bulte JWM. Fluorine ((19)F) MRS and MRI in biomedicine. NMR Biomed. 2011; 24:114–129. [PubMed: 20842758]
44. Cobb SL, Murphy CD. (19)F NMR applications in chemical biology. J Fluorine Chem. 2009; 130:132–143.
45. Dalvit C, Mongelli N, Papeo G, Giordano P, Veronesi M, Moskau D, Kummerle R. Sensitivity improvement in F-19 NMR-based screening experiments: Theoretical considerations and experimental applications. J Am Chem Soc. 2005; 127:13380–13385. [PubMed: 16173772]
46. Higuchi M, Iwata N, Matsuba Y, Sato K, Sasamoto K, Saido TC. F-19 and H-1 MRI detection of amyloid beta plaques in vivo. Nat Neurosci. 2005; 8:527–533. [PubMed: 15768036]
47. Dalvit C. Ligand- and substrate-based F-19 NMR screening: Principles and applications to drug discovery. Prog Nucl Magn Reson Spectrosc. 2007; 51:243–271.
48. Hammill JT, Miyake-Stoner S, Hazen JL, Jackson JC, Mehl RA. Preparation of site-specifically labeled fluorinated proteins for F-19-NMR structural characterization. Nat Protoc. 2007; 2:2601–2607. [PubMed: 17948003]
49. Papeo G, Giordano P, Brasca MG, Buzzo F, Caronni D, Ciprandi F, Mongelli N, Veronesi M, Vulpetti A, Dalvit C. Polyfluorinated amino acids for sensitive F-19 NMR-based screening and kinetic measurements. J Am Chem Soc. 2007; 129:5665–5672. [PubMed: 17417847]
50. Du WJ, Nystrom AM, Zhang L, Powell KT, Li YL, Cheng C, Wickline SA, Wooley KL. Amphiphilic Hyperbranched Fluoropolymers as Nanoscopic F-19 Magnetic Resonance Imaging Agent Assemblies. Biomacromolecules. 2008; 9:2826–2833. [PubMed: 18795785]
51. Stockman BJ. 2-fluoro-ATP as a versatile tool for F-19 NMR-based activity screening. J Am Chem Soc. 2008; 130:5870–5871. [PubMed: 18407634]
52. Ieronimo M, Afonin S, Koch K, Berditsch M, Wadhwani P, Ulrich AS. F-19 NMR Analysis of the Antimicrobial Peptide PGLa Bound to Native Cell Membranes from Bacterial Protoplasts and Human Erythrocytes. J Am Chem Soc. 2010; 132:8822–8824. [PubMed: 20550126]
53. Kiviniemi A, Virta P. Characterization of RNA Invasion by (19)F NMR Spectroscopy. J Am Chem Soc. 2010; 132:8560–8562. [PubMed: 20521791]
54. Li C, Wang GF, Wang Y, Creager-Allen R, Lutz EA, Scronce H, Slade KM, Ruf RAS, Mehl RA, Pielak GJ. Protein (19)F NMR in Escherichia coli. J Am Chem Soc. 2010; 132:321–327. [PubMed: 20050707]
55. Thurecht KJ, Blakey I, Peng H, Squires O, Hsu S, Alexander C, Whittaker AK. Functional Hyperbranched Polymers: Toward Targeted in Vivo F-19 Magnetic Resonance Imaging Using Designed Macromolecules. J Am Chem Soc. 2010; 132:5336–5337. [PubMed: 20345132]
56. Jiang ZX, Feng Y, Yu YB. Fluorinated paramagnetic chelates as potential multi-chromic (19)F tracer agents. Chem Commun. 2011; 47:7233–7235.
57. Takaoka Y, Kiminami K, Mizusawa K, Matsuo K, Narazaki M, Matsuda T, Hamachi I. Systematic Study of Protein Detection Mechanism of Self-Assembling 19F NMR/MRI Nanoprobes toward Rational Design and Improved Sensitivity. J Am Chem Soc. 2011; 133:11725–11731. [PubMed: 21699190]
58. Matsushita H, Mizukami S, Mori Y, Sugihara F, Shirakawa M, Yoshioka Y, Kikuchi K. 19F MRI Monitoring of Gene Expression in Living Cells through Cell-Surface b-Lactamase Assay. ChemBioChem. 2012; 13:1579–1583. [PubMed: 22777922]

59. Li FH, Shi P, Li JS, Yang F, Wang TY, Zhang W, Gao F, Ding W, Li D, Li J, Xiong Y, Sun JP, Gong WM, Tian CL, Wang JY. A Genetically Encoded F-19 NMR Probe for Tyrosine Phosphorylation. Angew Chem, Int Ed. 2013; 52:3958–3962.
60. Marsh ENG, Suzuki Y. Using 19F NMR to Probe Biological Interactions of Proteins and Peptides. ACS Chem Biol. 2014; 9:1242–1250. [PubMed: 24762032]
61. Tirotta I, Dichiarante V, Pigliacelli C, Cavallo G, Terraneo G, Bombelli FB, Metrangolo P, Resnati G. F-19 Magnetic Resonance Imaging (MRI): From Design of Materials to Clinical Applications. Chem Rev. 2015; 115:1106–1129. [PubMed: 25329814]
62. Gee CT, Koleski EJ, Pomerantz WCK. Fragment Screening and Druggability Assessment for the CBP/p300 KIX Domain through Protein-Observed F-19 NMR Spectroscopy. Angew Chem, Int Ed. 2015; 54:3735–3739.
63. Kitevski-LeBlanc JL, Prosser RS. Current applications of F-19 NMR to studies of protein structure and dynamics. Prog Nucl Magn Reson Spectrosc. 2012; 62:1–33. [PubMed: 22364614]
64. Chen H, Viel S, Ziarelli F, Peng L. F-19 NMR: a valuable tool for studying biological events. Chem Soc Rev. 2013; 42:7971–7982. [PubMed: 23864138]
65. Ye YS, Liu XL, Zhang ZT, Wu Q, Jiang B, Jiang L, Zhang X, Liu ML, Pielak GJ, Li CG. F-19 NMR Spectroscopy as a Probe of Cytoplasmic Viscosity and Weak Protein Interactions in Living Cells. Chem Eur J. 2013; 19:12705–12710. [PubMed: 23922149]
66. Yu JX, Hallac RR, Chiguru S, Mason RP. New frontiers and developing applications in F-19 NMR. Prog Nucl Magn Reson Spectrosc. 2013; 70:25–49. [PubMed: 23540575]
67. Ye YS, Liu XL, Xu GH, Liu ML, Li CG. Direct Observation of Ca2+-Induced Calmodulin Conformational Transitions in Intact Xenopus laevis Oocytes by F-19 NMR Spectroscopy. Angew Chem, Int Ed. 2015; 54:5328–5330.
68. Pomerantz WC, Wang N, Lipinski AK, Wang R, Cierpicki T, Mapp AK. Profiling the dynamic interfaces of fluorinated transcription complexes for ligand discovery and characterization. ACS Chem Biol. 2012; 7:1345–1350. [PubMed: 22725662]
69. Marsh ENG. Towards the nonstick egg: designing fluorous proteins. Chem Biol. 2000; 7:R153–R157. [PubMed: 10903940]
70. Yoder NC, Kumar K. Fluorinated amino acids in protein design and engineering. Chem Soc Rev. 2002; 31:335–341. [PubMed: 12491748]
71. Jäckel C, Koksch B. Fluorine in peptide design and protein engineering. Eur J Org Chem. 2005:4483–4503.
72. Merkel L, Schauer M, Antranikian G, Budisa N. Parallel Incorporation of Different Fluorinated Amino Acids: On the Way to “Teflon” Proteins. ChemBioChem. 2010; 11:1505–1507. [PubMed: 20572253]
73. Qiu XL, Qing FL. Recent Advances in the Synthesis of Fluorinated Amino Acids. Eur J Org Chem. 2011:3261–3278.
74. Salwiczek M, Nyakatura EK, Gerling UIM, Ye SJ, Koksch B. Fluorinated amino acids: compatibility with native protein structures and effects on protein-protein interactions. Chem Soc Rev. 2012; 41:2135–2171. [PubMed: 22130572]
75. Pandey AK, Naduthambi D, Thomas KM, Zondlo NJ. Proline Editing: A General and Practical Approach to the Synthesis of Functionally and Structurally Diverse Peptides. Analysis of Steric versus Stereoelectronic Effects of 4-Substituted Prolines on Conformation within Peptides. J Am Chem Soc. 2013; 135:4333–4363. [PubMed: 23402492]
76. Odar C, Winkler M, Wiltschi B. Fluoro amino acids: A rarity in nature, yet a prospect for protein engineering. Biotechnol J. 2015; 10:427–446. [PubMed: 25728393]
77. Bilgicer B, Fichera A, Kumar K. A coiled coil with a fluorous core. J Am Chem Soc. 2001; 123:4393–4399. [PubMed: 11457223]
78. Bilgicer B, Xing X, Kumar K. Programmed self-sorting of coiled coils with leucine and hexafluoroleucine cores. J Am Chem Soc. 2001; 123:11815–11816. [PubMed: 11716746]
79. Tang Y, Tirrell DA. Biosynthesis of a Highly Stable Coiled-Coil Protein Containing Hexafluoroleucine in an Engineered Bacterial Host. J Am Chem Soc. 2001; 123:11089–11090. [PubMed: 11686725]

80. Wang P, Tang Y, Tirrell DA. Incorporation of trifluoroisoleucine into proteins in vivo. J Am Chem Soc. 2003; 125:6900–6906. [PubMed: 12783542]
81. Lee KH, Lee HY, Slutsky MM, Anderson JT, Marsh ENG. Fluorous effect in proteins: De novo design and characterization of a four-alpha-helix bundle protein containing hexafluoroleucine. Biochemistry. 2004; 43:16277–16284. [PubMed: 15610021]
82. Luo ZY, Zhang QS, Oderaotoshi Y, Curran DP. Fluorous mixture synthesis: A fluorous-tagging strategy for the synthesis and separation of mixtures of organic compounds. Science. 2001; 291:1766–1769. [PubMed: 11230688]
83. Buer BC, Meagher JL, Stuckey JA, Marsh ENG. Structural basis for the enhanced stability of highly fluorinated proteins. Proc Natl Acad Sci USA. 2012; 109:4810–4815. [PubMed: 22411812]
84. Link AJ, Mock ML, Tirrell DA. Non-canonical amino acids in protein engineering. Curr Opin Biotech. 2003; 14:603–609. [PubMed: 14662389]
85. Johnson JA, Lu YY, Van Deventer JA, Tirrell DA. Residue-specific incorporation of non-canonical amino acids into proteins: recent developments and applications. Curr Opin Chem Biol. 2010; 14:774–780. [PubMed: 21071259]
86. Renner C, Alefelder S, Bae JH, Budisa N, Huber R, Moroder L. Fluoroprolines as Tools for Protein Design and Engineering. Angew Chem, Int Ed. 2001; 40:923–925.
87. Bretscher LE, Jenkins CL, Taylor KM, DeRider ML, Raines RT. Conformational Stability of Collagen Relies on a Stereoelectronic Effect. J Am Chem Soc. 2001; 123:777–778. [PubMed: 11456609]
88. Jackel C, Salwiczek M, Koksch B. Fluorine in a native protein environment - How the spatial demand and polarity of fluoroalkyl groups affect protein folding. Angew Chem Int Ed. 2006; 45:4198–4203.
89. Kim W, Hardcastle KI, Conticello VP. Fluoroproline flip-flop: Regiochemical reversal of a stereoelectronic effect on peptide and protein structures. Angew Chem, Int Ed. 2006; 45:8141–8145.
90. Buer BC, de la Salud-Bea R, Hashimi HMA, Marsh ENG. Engineering Protein Stability and Specificity Using Fluorous Amino Acids: The Importance of Packing Effects. Biochemistry. 2009; 48:10810–10817. [PubMed: 19824630]
91. Baker PJ, Montclare JK. Enhanced Refoldability and Thermoactivity of Fluorinated Phosphotriesterase. ChemBioChem. 2011; 12:1845–1848. [PubMed: 21710682]
92. Pace CJ, Zheng H, Mylvaganam R, Kim D, Gao JM. Stacked Fluoroaromatics as Supramolecular Synthons for Programming Protein Dimerization Specificity. Angew Chem, Int Ed. 2012; 51:103–107.
93. Roderer D, Glockshuber R, Rubini M. Acceleration of the Rate-Limiting Step of Thioredoxin Folding by Replacement of its Conserved cis-Proline with (4S)-Fluoroproline. ChemBioChem. 2015; 16:2162–2166. [PubMed: 26382254]
94. Jackson JC, Hammill JT, Mehl RA. Site-specific incorporation of a F-19-amino acid into proteins as an NMR probe for characterizing protein structure and reactivity. J Am Chem Soc. 2007; 129:1160–1166. [PubMed: 17263397]
95. Chiu HP, Suzuki Y, Gullickson D, Ahmad R, Kokona B, Fairman R, Cheng RP. Helix Propensity of Highly Fluorinated Amino Acids. J Am Chem Soc. 2006; 128:15556–15557. [PubMed: 17147342]
96. Chiu HP, Kokona B, Fairman R, Cheng RP. Effect of Highly Fluorinated Amino Acids on Protein Stability at a Solvent-Exposed Position on an Internal Strand of Protein G B1 Domain. J Am Chem Soc. 2009; 131:13192–13192. [PubMed: 19711980]
97. Horng JC, Raleigh DP. Phi-Values beyond the ribosomally encoded amino acids: Kinetic and thermodynamic consequences of incorporating trifluoromethyl amino acids in a globular protein. J Am Chem Soc. 2003; 125:9286–9287. [PubMed: 12889945]
98. Nyakatura EK, Reimann O, Vagt T, Salwiczek M, Koksch B. Accommodating fluorinated amino acids in a helical peptide environment. RSC Adv. 2013; 3:6319–6322.
99. Gerling UIM, Salwiczek M, Cadicamo CD, Erdbrink H, Czekelius C, Grage SL, Wadhwani P, Ulrich AS, Behrends M, Haufe G, Koksch B. Fluorinated amino acids in amyloid formation: a symphony of size, hydrophobicity and alpha-helix propensity. Chem Sci. 2014; 5:819–830.

100. Tressler CM, Zondlo NJ. (2S,4R)- and (2S,4S)-Perfluoro-tert-butyl 4-Hydroxyproline: Two Conformationally Distinct Proline Amino Acids for Sensitive Application in 19F NMR. J Org Chem. 2014; 79:5880–5886. [PubMed: 24870929]
101. Jiang ZX, Yu YB. The synthesis of a geminally perfluoro-tert-butylated beta-amino acid and its protected forms as a potential pharmacokinetic modulator and reporter for peptide-based pharmaceuticals. J Org Chem. 2007; 72:1464–1467. [PubMed: 17243713]
102. Buer BC, Levin BJ, Marsh ENG. Perfluoro-tert-butyl-homoserine as a sensitive F-19 NMR reporter for peptide-membrane interactions in solution. J Pept Sci. 2013; 19:308–314. [PubMed: 23509011]
103. Yue X, Taraban MB, Hyland LL, Yu YB. Avoiding Steric Congestion in Dendrimer Growth through Proportionate Branching: A Twist on da Vinci's Rule of Tree Branching. J Org Chem. 2012; 77:8879–8887. [PubMed: 23039185]
104. Tressler CM, Zondlo NJ. Synthesis of Perfluoro-tert-butyl Tyrosine, for Applications in 19F NMR, via a Diazonium Coupling Reaction. Org Lett. 2016; 18:6240–6243. [PubMed: 27978684]
105. Brown AM, Zondlo NJ. A Propensity Scale for Type II Polyproline Helices (PPII): Aromatic Amino Acids in Proline-Rich Sequences Strongly Disfavor PPII Due to Proline-Aromatic Interactions. Biochemistry. 2012; 51:5041–5051. [PubMed: 22667692]
106. Elbaum MB, Zondlo NJ. OGlcNAcylation and Phosphorylation Have Similar Structural Effects in α-Helices: Post-Translational Modifications as Inducible Start and Stop Signals in α-Helices, with Greater Structural Effects on Threonine Modification. Biochemistry. 2014; 53:2242–2260. [PubMed: 24641765]
107. Vuister GW, Bax A. Quantitative J Correlation: A New Approach for Measuring Homonuclear Three-Bond $J_{HNH\alpha}$ Coupling Constants in ^{15}N-enriched Proteins. J Am Chem Soc. 1993; 115:7772–7777.
108. Wishart DS, Sykes BD, Richards FM. Relationship between nuclear magnetic resonance chemical shift and protein secondary structure. J Mol Biol. 1991; 222:311–333. [PubMed: 1960729]
109. Wishart DS, Sykes BD, Richards FM. The chemical shift index: a fast and simple method for the assignment of protein secondary structure through NMR spectroscopy. Biochemistry. 1992; 31:1647–1651. [PubMed: 1737021]
110. Wishart DS, Sykes BD. The C-13 Chemical Shift Index - A Simple Method for the Identification of Protein Secondary Structure Using C-13 Chemical-Shift Data. J Biomol NMR. 1994; 4:171–180. [PubMed: 8019132]
111. Sebesta DP, Orourke SS, Pieken WA. Facile preparation of perfluoro-tert-butyl ethers by the Mitsunobu reaction. J Org Chem. 1996; 61:361–362.
112. Luo PZ, Baldwin RL. Mechanism of helix induction by trifluoroethanol: A framework for extrapolating the helix-forming properties of peptides from trifluoroethanol/water mixtures back to water. Biochemistry. 1997; 36:8413–8421. [PubMed: 9204889]
113. Rohl CA, Baldwin RL. Comparison of NH Exchange and Circular Dichroism as Techniques for Measuring the Parameters of the Helix-Coil Transition in Peptides. Biochemistry. 1997; 36:8435–8442. [PubMed: 9214287]
114. Presta LG, Rose GD. Helix Signals in Proteins. Science. 1988; 240:1632–1641. [PubMed: 2837824]
115. Richardson JS, Richardson DC. Amino-Acid Preferences for Specific Locations at the Ends of Alpha-Helices. Science. 1988; 240:1648–1652. [PubMed: 3381086]
116. Cochran DAE, Penel S, Doig AJ. Effect of the N1 residue on the stability of the alpha-helix for all 20 amino acids. Protein Sci. 2001; 10:463–470. [PubMed: 11344315]
117. Kemp DS, Allen TJ, Oslick SL. The Energetics of Helix Formation by Short Templated Peptides in Aqueous Solution. 1 Characterization of the Reporting Helical Template Ac-Hel_1. J Am Chem Soc. 1995; 117:6641–6657.
118. Pace CN, Scholtz JM. A helix propensity scale based on experimental studies of peptides and proteins. Biophys J. 1998; 75:422–427. [PubMed: 9649402]
119. Adzhubei AA, Sternberg MJE. Left-Handed Polyproline-II Helices Commonly Occur in Globular-Proteins. J Mol Biol. 1993; 229:472–493. [PubMed: 8429558]

120. Adzhubei AA, Sternberg MJE, Makarov AA. Polyproline-II Helix in Proteins: Structure and Function. J Mol Biol. 2013; 425:2100–2132. [PubMed: 23507311]

121. Shi ZS, Woody RW, Kallenbach NR. Is polyproline II a major backbone conformation in unfolded proteins? Adv Protein Chem. 2002; 62:163–240. [PubMed: 12418104]

122. Ding L, Chen K, Santini PA, Shi Z, Kallenbach NR. The Pentapeptide GGAGG Has PII Conformation. J Am Chem Soc. 2003; 125:8092–8093. [PubMed: 12837065]

123. Rucker AL, Pager CT, Campbell MN, Qualls JE, Creamer TP. Host-Guest Scale of Left-Handed Polyproline II Helix Formation. Proteins. 2003; 53:68–75. [PubMed: 12945050]

124. Chen K, Liu ZG, Zhou CH, Shi ZS, Kallenbach NR. Neighbor effect on PPII conformation in alanine peptides. J Am Chem Soc. 2005; 127:10146–10147. [PubMed: 16028907]

125. Shi Z, Chen K, Liu Z, Ng A, Bracken WC, Kallenbach NR. Polyproline II propensities from GGXGG peptides reveal an anticorrelation with b-sheet scales. Proc Natl Acad Sci USA. 2005; 102:17964–17968. [PubMed: 16330763]

126. Pandey AK, Thomas KM, Forbes CR, Zondlo NJ. Tunable Control of Polyproline Helix (PPII) Structure via Aromatic Electronic Effects: An Electronic Switch of Polyproline Helix. Biochemistry. 2014; 53:5307–5314. [PubMed: 25075447]

127. Dunbrack RL Jr, Karplus M. Backbone-dependent Rotamer Library for Proteins: Application to Side-chain prediction. J Mol Biol. 1993; 230:543–574. [PubMed: 8464064]

128. Lovell SC, Word JM, Richardson JS, Richardson DC. The Penultimate Rotamer Library. Proteins. 2000; 40:389–408. [PubMed: 10861930]

129. Galande AK, Bramlett KS, Trent JO, Burris TP, Wittliff JL, Spatola AF. Potent Inhibitors of LXXLL-Based Protein– Protein Interactions. ChemBioChem. 2005; 6:1991–1998. [PubMed: 16222726]

130. Melcher K. The strength of acidic activation domains correlates with their affinity for both transcriptional and non-transcriptional proteins. J Mol Biol. 2000; 301:1097–1112. [PubMed: 10966808]

131. Gee AC, Carlson KE, Martini PGV, Katzenellenbogen BS, Katzenellenbogen JA. Coactivator Peptides Have a Differential Stabilizing Effect on the Binding of Estrogens and Antiestrogens with the Estrogen Receptor. Mol Endocrinol. 1999; 13:1912–1923. [PubMed: 10551784]

132. Zhao L, Chmielewski J. Inhibiting protein-protein interactions using designed molecules. Curr Opin Struct Biol. 2005; 15:31–34. [PubMed: 15718130]

133. Yu LP, Hajduk PJ, Mack J, Olejniczak ET. Structural studies of Bcl-xL/ligand complexes using F-19 NMR. J Biomol NMR. 2006; 34:221–227. [PubMed: 16645812]

134. Arntson KE, Pomerantz WCK. Protein-Observed Fluorine NMR: A Bioorthogonal Approach for Small Molecule Discovery. J Med Chem. 2016; 59:5158–5171. [PubMed: 26599421]

135. Tengel T, Fex T, Emtenas H, Almqvist F, Sethson I, Kihlberg J. Use of F-19 NMR spectroscopy to screen chemical libraries for ligands that bind to proteins. Org Biomol Chem. 2004; 2:725–731. [PubMed: 14985813]

136. Mizukami S, Takikawa R, Sugihara F, Hori Y, Tochio H, Walchli M, Shirakawa M, Kikuchi K. Paramagnetic relaxation-based F-19 MRI probe to detect protease activity. J Am Chem Soc. 2008; 130:794–795. [PubMed: 18154336]

137. Kitevski-LeBlanc JL, Evanics F, Prosser RS. Approaches for the measurement of solvent exposure in proteins by F-19 NMR. J Biomol NMR. 2009; 45:255–264. [PubMed: 19655092]

138. Wang GF, Li CG, Pielak GJ. (19)F NMR studies of alpha-synuclein-membrane interactions. Prot Sci. 2010; 19:1686–1691.

139. Jensen MR, Ruigrok RWH, Blackledge M. Describing intrinsically disordered proteins at atomic resolution by NMR. Curr Opin Struct Biol. 2013; 23:426–435. [PubMed: 23545493]

140. Kragelj J, Ozenne V, Blackledge M, Jensen MR. Conformational Propensities of Intrinsically Disordered Proteins from NMR Chemical Shifts. ChemPhysChem. 2013; 14:3034–3045. [PubMed: 23794453]

141. Brister MA, Pandey AK, Bielska AA, Zondlo NJ. OGlcNAcylation and Phosphorylation Have Opposing Structural Effects in tau: Phosphothreonine Induces Particular Conformational Order. J Am Chem Soc. 2014; 136:3803–3816. [PubMed: 24559475]

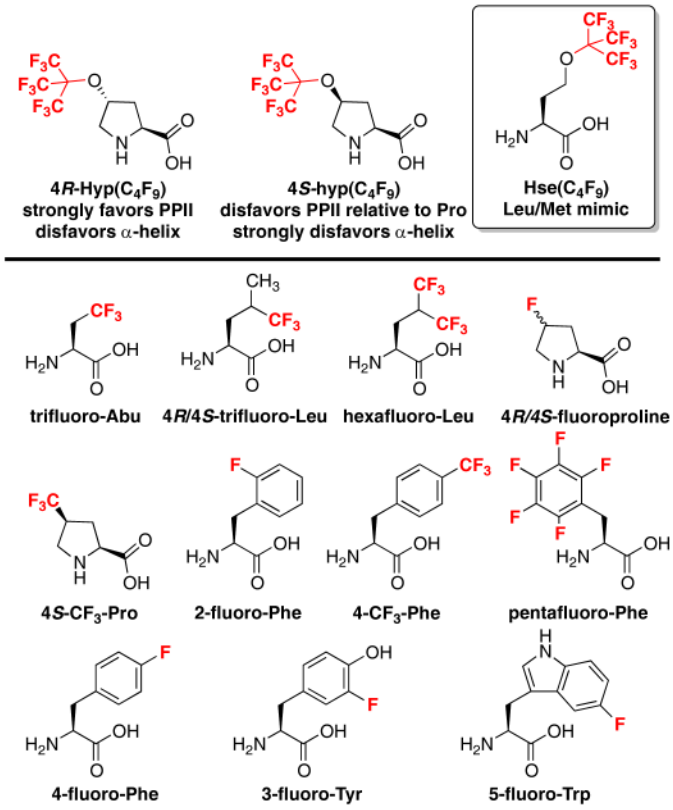

Figure 1.

Top: perfluoro-*tert*-butyl amino acids; bottom: selected aliphatic and aromatic fluorinated amino acids used for ^{19}F NMR-based detection.

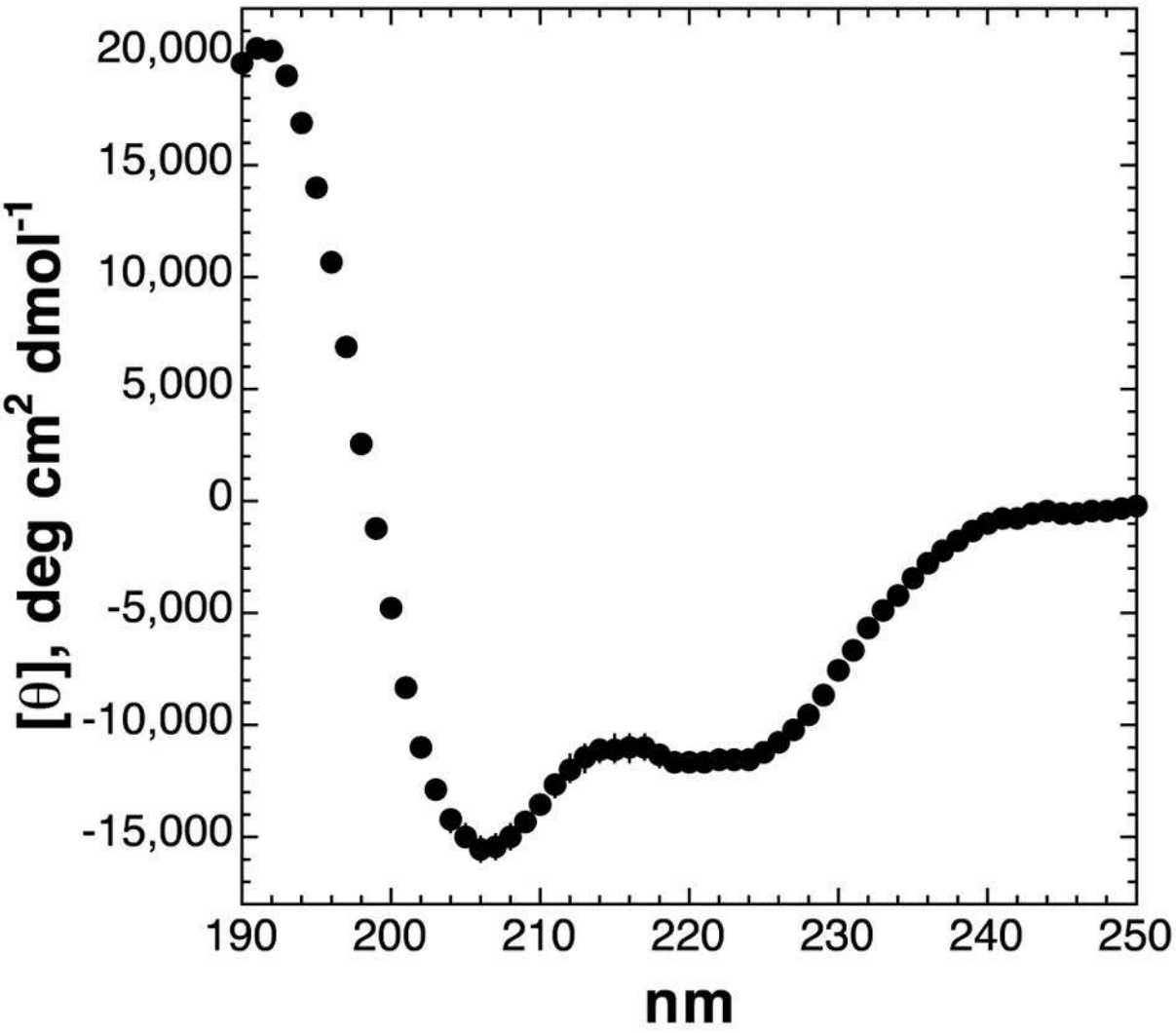

Figure 2.

CD spectrum of Ac-(**Hse(C_4F_9)**)KAAAAKAAAAKAAGY-NH_2 in the Baldwin-type α-helical model peptide previously employed(100, 106) to determine the structural effects of serine and threonine phosphorylation and O-GlcNAcylation on α-helix stability. Experiments were conducted in 5 mM phosphate buffer with 25 mM KF at pH 7.4 at 0.5 °C. Extent of α-helical structure is indicated by $[\theta]_{222} = -11510 \pm 400$ deg cm^2 $dmol^{-1}$, $[\theta]_{222}/[\theta]_{208} = 0.77$, corresponding to 36% α-helix.(112, 113) Error bars are shown and indicate standard error. The $^3J_{\alpha N}$ (Figure S5), which correlates with the ϕ torsion angle (smaller value = more compact ϕ),(107) is 6.4 Hz for Hse(C_4F_9) in this peptide, similar to that of Thr (6.2 Hz) at this position in this peptide context, and greater than that of the more α-helical Ser (5.1 Hz) at this position in this peptide context.

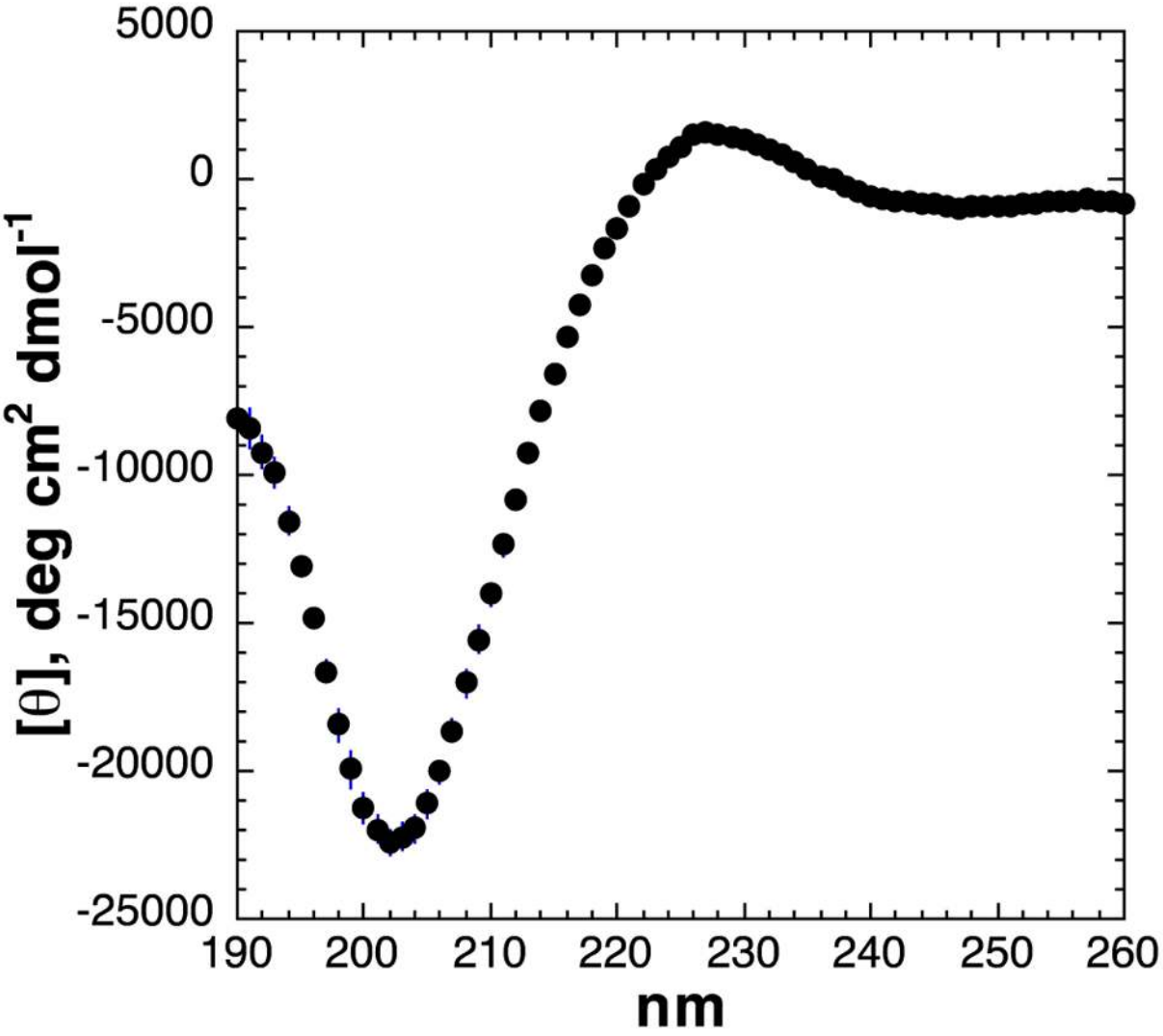

Figure 3.

CD spectrum of Ac-GPP(**Hse(C_4F_9)**)PPGY-NH_2 in the model peptide context previously employed(100, 105, 126, 141) to determine polyproline II helix propensities of guest amino acids at the indicated position of substitution. Experiments were conducted in 5 mM phosphate buffer with 25 mM KF at pH 7.4 at 25 °C. Extent of PPII is indicated by $[\theta]_{228}$ = 1500 ± 190 deg cm^2 $dmol^{-1}$. The $^3J_{\alpha N}$ for Hse(C_4F_9) is 7.7 Hz, compared to $^3J_{\alpha N}$ = 7.2 Hz for Met in this position in this peptide context.

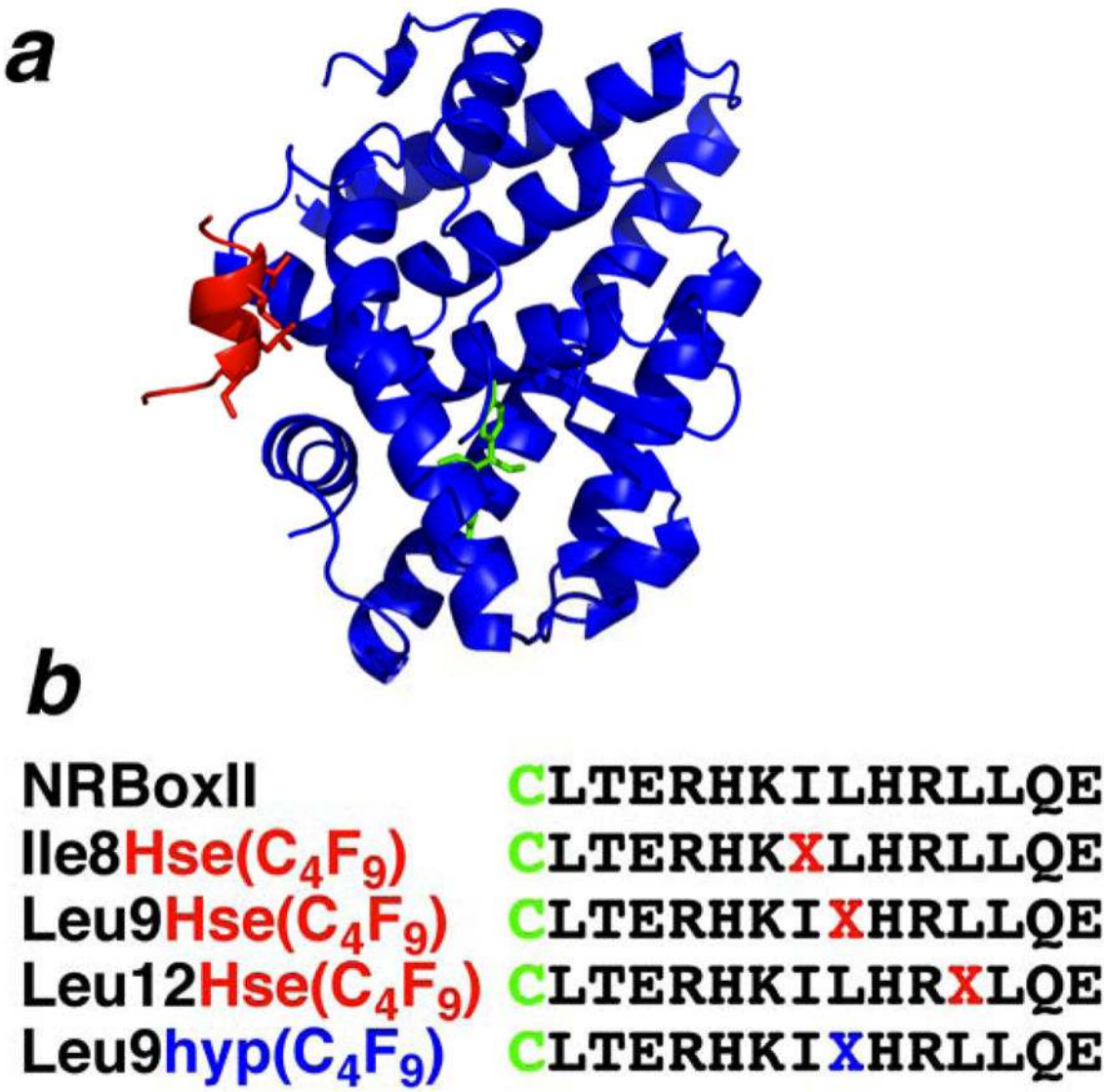

Figure 4.

(a) X-ray crystal structure (pdb 3erd)(22) of the estrogen receptor-α ligand-binding domain (ERα LBD, residues 305-550, blue) bound to the estrogen mimic diethylstilbestrol (green) and the GRIP1 NRBoxII co-activator peptide (HK**IL**HR**LL**QDS, red). Coactivator peptides bind to the ligand-bound estrogen receptor via one face of an α-helix containing the LXXLL short linear motif (side chains shown). (b) Peptide designs for the incorporation of perfluoro-*tert*-butyl amino acids into estrogen receptor coactivator peptides. X indicates the site of modification with a perfluoro-*tert*-butyl amino acid, with either Hse(C_4F_9) (red) or 4*S*-hyp(C_4F_9) (blue) substitution at the indicated residue. All peptides for fluorescence polarization experiments were labeled with 5-iodoacetamidofluorescein on Cys (green). Peptides used in NMR spectroscopy experiments lacked the N-terminal Cys. All peptides were acetylated on the N-terminus and contain C-terminal amides. Details of the synthesis and characterization of peptides are in the Supporting Information.

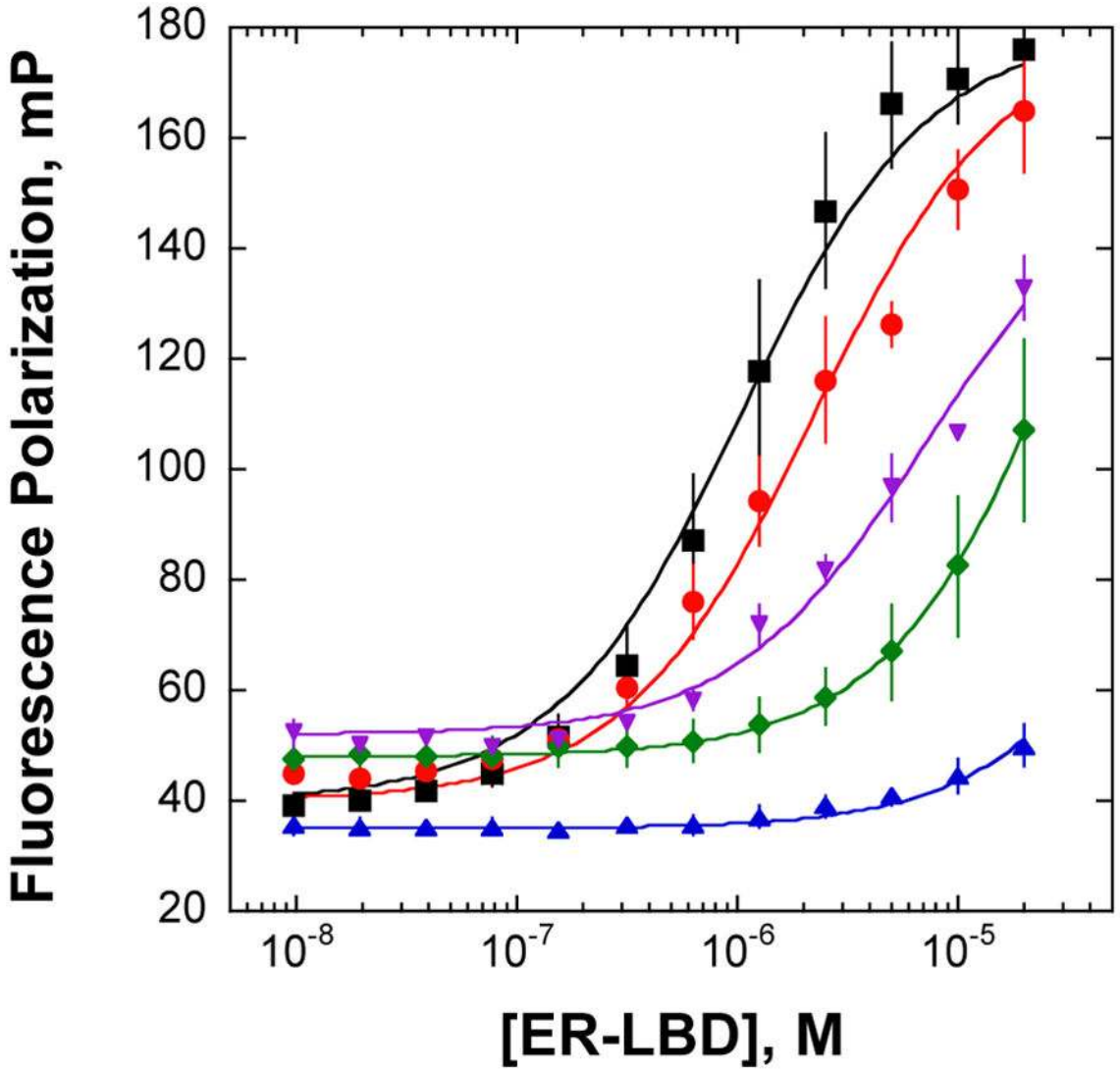

Figure 5.

Binding isotherms of estradiol-bound ERα LBD to the fluorescein-labeled peptides NRBoxII (black squares), Leu12Hse(C_4F_9) (red circles), Ile8Hse(C_4F_9) (magenta inverted triangles), Leu9Hse(C_4F_9) (green diamonds), and Leu9hyp(C_4F_9) (blue triangles). Assays were conducted using 100 nM fluorescein-labeled peptides in 1× PBS buffer (pH 7.4) with 20 μM estradiol, 0.1 mM DTT, and 0.04 mg/mL BSA. ERα LBD was diluted using two-fold serial dilutions to final protein concentrations of 10 μM to 0.0098 μM. Fluorescence polarization data represent the average of at least 3 independent trials. Polarization data are in millipolarization units (mP). Each data point is indicative of at least three independent trials. Error bars indicate standard error.

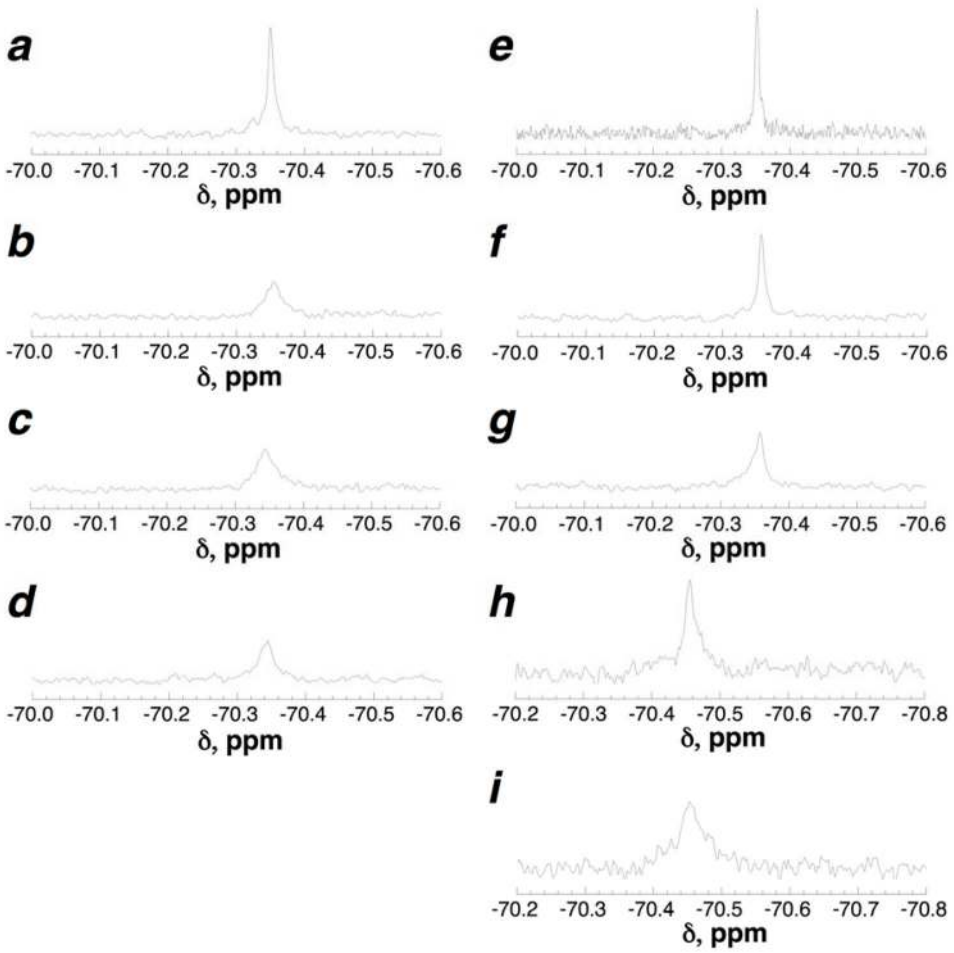

Figure 6.

^{19}F NMR spectroscopy of the peptide Leu12Hse(C_4F_9). Experiments were conducted with 5 μM peptide in 1× PBS (pH 7.4), 0.1 mM DTT, 20 μM estradiol (except g), and 10% D_2O. (a–e) The peptide Leu12Hse(C_4F_9) with (a) no added protein; (b) 5 μM ERα LBD; (c) 15 μM ERα LBD; (d) 30 μM ERα LBD; and (e) 30 μM bovine gamma globulin. (f) 5 μM peptide Leu12Hse(C_4F_9) with 15 μM ERα LBD and 20 μM NRBox II. (g) 5 μM peptide Leu12Hse(C_4F_9) with 15 μM ERα LBD and 50 μM 4-hydroxytamoxifen (OHT), without added estradiol. (h–i) The peptide Leu12Hse(C_4F_9) (h) with 200 μL HeLa cell lysates and (i) with 200 μL HeLa cell lysates and 15 μM ERα LBD (final concentration). All ^{19}F NMR spectra were acquired with a 10 ppm sweep width, acquisition time = 0.8 seconds, 1024 scans, and a relaxation delay of 3.0 seconds. Comparable data acquired in independent experiments with 128 scans (8 minute experiment time) are in the Supporting Information (Figure S22). Figures 6a–6g have identical scales on the y-axes.

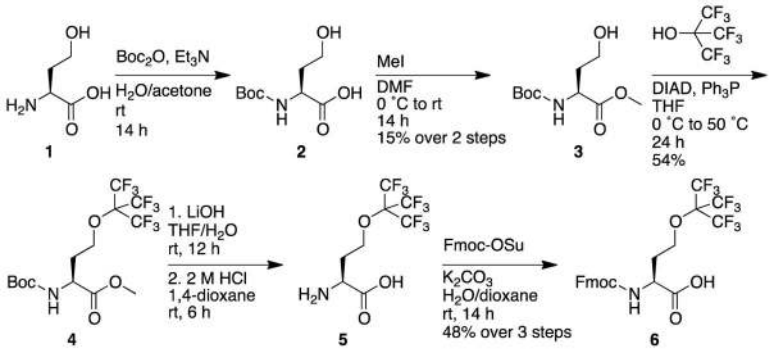

Scheme 1.

Synthesis of Fmoc-perfluoro-*tert*-butyl homoserine (**6**) from homoserine (**1**). **2** is also commercially available.

Table 1

Circular dichroism data for peptides with the indicated guest residues **X** in the α-helical model peptide host system Ac-**X**KAAAAKAAAAKAAGY-NH_2. Extent of α-helix is identified by mean residue ellipticity at 222 nm ($[\theta]_{222}$) or via the ratios $[\theta]_{222}/[\theta]_{208}$ or $-[\theta]_{190}/[\theta]_{222}$. % α-Helix was determined via the method of Baldwin,(112, 113) as described previously.(106) Ser and Thr are highly stabilizing to α-helices at their N-terminus due to the possibility of hydrogen bonding with unsatisfied amide N-H hydrogen bond donors. (114–116)

X =	$[\theta]_{222}$ deg cm^2 $dmol^{-1}$	$[\theta]_{208}$ deg cm^2 $dmol^{-1}$	$[\theta]_{190}$ deg cm^2 $dmol^{-1}$	$[\theta]_{222}/[\theta]_{208}$	$-[\theta]_{190}/[\theta]_{222}$	% α-helix
Ser[a]	−16620	−16430	32240	1.01	1.96	50%
Thr[a]	−14860	−15420	27160	0.96	1.76	45%
Pro[a]	−12030	−13890	16190	0.87	1.17	38%
Hse(C_4F_9)	−11510	−14960	19520	0.77	1.70	36%
Hyp(C_4F_9)[b]	−6840	−11040	7380	0.67	1.08	24%
hyp(C_4F_9)[b]	−4990	−7850	5090	0.64	1.01	19%

[a]Reference (106)

[b]Reference (100)

Table 2

Circular dichroism data for peptides with the indicated guest residues **X** in the polyproline helix model peptide host system(105) Ac-GPP**X**PPGY-NH_2. Extent of polyproline helix is identified by mean residue ellipticity at 228 nm ($[\theta]_{228}$), with more positive numbers indicating greater extent of polyproline helix.

X =	**$[\theta]_{228}$ deg cm^2 $dmol^{-1}$**
Hyp(C_4F_9)	3370[a]
Pro	2950[b]
Leu	2230[b]
hyp(C_4F_9)	1700[a]
Hse(C_4F_9)	1500
Hse	1390[b]
Met	1380[b]
Ser	460[b]
Val	−120[b]
tert-Leu	−940[b]

[a]Reference (100)

[b]Reference (105)

Table 3

Dissociation constants (K_d) for the complexes of estradiol-bound ERα LBD and the indicated peptides. Errors indicate standard error. K_d values were determined via a non-linear least-squares fit to the fluorescence polarization data. n.a. not applicable.

peptide	K_d, μM	error, μM	ΔG, kcal mol^{-1}
NRBoxII	1.0	0.1	−8.2
Ile8Hse(C_4F_9)	7.1	1.3	−7.0
Leu9Hse(C_4F_9)	43	4	−6.0
Leu12Hse(C_4F_9)	2.2	0.2	−7.7
Leu9hyp(C_4F_9)	>150	n.a.	n.a.